Received: 2 March 2021 | Revised: 5 May 2021 | Accepted: 11 May 2021

DOI: 10.1002/pc.26136

RESEARCH ARTICLE

Polymer COMPOSITES WILEY

Using infrared spectroscopy in combination with multivariate data analysis to predict residual strength of carbon fiber reinforced polymers after one-sided thermal loading

Tanja Marina Vetter[1,2] | **Felix Zimmer**[2] | **Sebastian Eibl**[2] | **Hans-Joachim Gudladt**[1]

[1]Department of Aerospace Engineering, Universität der Bundeswehr München, Neubiberg, Germany

[2]Chemistry of Materials and POL, Environmental Protection, Bundeswehr Research Institute for Materials, Fuels and Lubricants (WIWeB), Erding, Germany

Correspondence
Tanja Marina Vetter, Department of Aerospace Engineering, Universität der Bundeswehr München, Werner-Heisenberg-Weg 39, 85577 Neubiberg, Germany.
Email: tanjavetter@bundeswehr.org

Abstract

In this study, structural, mechanical, and chemical changes of one-sided thermally loaded carbon fiber reinforced polymers (CFRPs) are investigated. The aim is to test and reliably predict residual strength and delamination depth by using infrared spectroscopy. CFRP of different thicknesses (HexPly® 8552/IM7) were irradiated at varying heat fluxes over various time intervals. The inhomogeneously distributed matrix degradation was analyzed by means of attenuated total reflection Fourier transform infrared spectroscopy with a depth resolution of 0.2 mm. Residual interlaminar shear strength (ILSS) was determined and microfocused computed X-ray tomography was used to measure the delamination depth. Principal component analyses were performed to show which information in the infrared spectra is affected by thermal loading. Furthermore, the combination of spectra taken at different depths of the CFRP can be used to develop partial least squares regression models to predict ILSS and delamination depth. Despite an inhomogenous distribution of thermal damage, precise predictions of ILSS and delamination depth with models considering varying sample thicknesses and heat fluxes were achieved.

KEYWORDS

ATR-FTIR spectroscopy, CFRP, chemometrics, ILSS, PLS, thermal damage

1 | INTRODUCTION

The application of carbon fiber reinforced polymers (CFRPs) is common practice in aerospace industry. CFRPs have the advantage of a higher strength-to-weight ratio compared to metal structures.[1] Conversely, CFRPs are less thermally stable. For example, thermal damage of CFRP occurs after uncontrolled heat development during repairs with hot-curing adhesives or overheating of electronic components. Thermally damaged CFRPs on only one side are especially difficult to characterize due to inhomogeneously distributed damage.[2–4] Consequently,

the knowledge about thermally induced degradation mechanisms and phenomena as well as their influence on residual strength is mandatory if CFRP shall be used despite thermal damage. Furthermore, the ability to predict thermal damage and residual strength directly on the damaged structure at an aircraft is desirable.

Thermal damage and the accompanying degradation phenomena can be characterized in different ways:

Micro attenuated total reflection Fourier transform infrared spectroscopy (ATR-FTIR) allows the degradation of the polymer matrix after thermal loading to be observed.[5–8] In the case of inhomogeneous thermal loading, measuring along a ground incline plane allows the distribution of matrix degradation inside the CFRP to be determined.[9] Hand-held spectrometers, which can be directly used on damaged aircraft structures, are especially attractive for the analysis of thermally damaged CFRP.[10,11] Furthermore, interlaminar shear strength (ILSS) testing is a convenient mechanical testing method due to its sensitive response to delaminations.[12–14] Lastly, the depth of delaminations can be resolved by means of microfocused computed X-ray tomography (μCT) with a good resolution in the micrometer scale. However, μCT cannot presently be used directly on damaged aircraft CFRP due to its complex device setup.[12,15] In order to analyze thermally induced structural damage directly, other nondestructive testing methods such as ultrasonic testing, laser shearography, or infrared thermography are available but with the limitations of a resolution in the millimeter-scale.[16,17] Here, only ultrasonic testing and infrared thermography allow the determination of delamination depths.

Damage investigations undertaken by Vetter et al. showed the coherence between decreasing non-delaminated thickness and decreasing residual ILSS of CFRP after one-sided thermal loading.[18] A reliable estimation of residual strength is only possible if the CFRP is penetrated with delaminations less than 50% of its sample thickness. Without an exact localization of the delamination depth within the CFRP, no statement about residual strength and a further usage of a structure is possible. This often leads to a complete replacement, which can be expensive and time intensive.[18] Therefore, an ability to reliably predict the residual strength after thermal loading is preferable, especially directly on the damaged aircraft.

Earlier investigations have shown that infrared spectroscopy in combination with multivariate regression methods like, for example, partial least squares regression (PLS), principal component regression, or artificial neural networks are powerful tools to predict residual strength of isothermally treated CFRP.[19–23] Wolfrum et al. established a PLS model for predicting ILSS after one-sided thermal loading at one heat-flux by using front or back side spectra.[24] Furthermore, classification models exist based on linear discriminant analysis that can predict if thermally induced delaminations are present or not.[25]

Ideally, PLS models are independent of influence parameters like, for example, sample thickness or heat flux. Unfortunately, modeling with increasing complexity of these parameters usually is accompanied with a decreasing prediction quality. Eibl discussed this difficulty for isothermally treated CFRP.[22] Here, the usage of spectra from one depth such as surface spectra to predict volume properties (e.g. ILSS) by means of PLS regression is possible because thermal damage is evenly distributed inside the CFRP. However, using only spectra from one depth to predict volume properties of one-sided thermally loaded CFRP includes a certain error rate due to the inhomogenous distribution of the damage. Therefore, the combination of spectra taken at different depths of the CFRP is believed to indicate the inhomogenous thermal damage inside the CFRP in PLS models and thus provide a more reliable prediction of volume properties. The aim of this work is to find the best combination of spectra by establishing PLS models with varying number and depths at which the spectra were taken as well as the distance between them to achieve an improved prediction quality and universal applicability.

2 | EXPERIMENTAL

2.1 | Material and thermal treatment

For this study, the commercially available CFRP HexPly® 8552/IM7 by Hexcel Corporation was used.[26] CFRP panels are produced with an unidirectional lay-up and a sample thickness z of 4 and 8 mm. These panels were sawed in samples with a size of 100×100 mm^2 and were subsequently irradiated with a conical heater of a cone calorimeter by Fire Testing Technology ltd. under different conditions. The irradiation times and heat for all samples are listed in Table 1. The temperature was measured with type K thermocouples laminated on the irradiated front side (T_{fs}) and on the back side (T_{bs}).

2.2 | Analytical methods

Micro ATR-FTIR spectroscopy was performed with a Bruker Tensor 27 spectrometer equipped with a Harrick ATR cell using a silicon crystal (diameter = 100 μm). For a depth-resolved analysis of matrix degradation, three spectra per depth were taken along a ground incline

TABLE 1 List of all tested CFRP samples and the associated heat flux, sample thickness (z), and irradiation time

Sample thickness z (mm)	Heat flux (kW/m^2)	Irradiation time (s)	ILSSτ (N/mm^2)	Delamination depth z_d (mm)	Front side temperature T_{fs} (°C)	Back side temperature T_{bs} (°C)
4	No thermal loading		104 ± 5.2	0	-	-
	15	60	109 ± 4.7	0	91	59
		180	108 ± 3.5	0	221	189
		300	105 ± 4.0	0	279	247
		600	85.6 ± 6.1	0	318	282
		900	70.0 ± 8.5	2.83	318	278
		1800	60.6 ± 9.6	3.04	318	276
	30	60	106 ± 4.4	0	197	140
		120	95.1 ± 6.6	0	311	248
		180	44.5 ± 7.8	3.83	392	240
		220	34.6 ± 6.0	4*	480	250
		240	28.1 ± 5.9	4*	487	242
	50	15	105 ± 5.2	0	202	108
		30	104 ± 5.2	0	261	165
		50	101 ± 5.0	0	330	227
		55	93.6 ± 4.7	0	343	241
		60	90.0 ± 4.5	0	361	258
		65	79.4 ± 4.0	0.47	375	273
		70	63.9 ± 3.2	1.48	392	285
		75	55.4 ± 2.8	2.16	412	295
		80	41.1 ± 2.1	3.59	437	307
8	No thermal loading		101 ± 2.9	0	-	-
	15	60	104 ± 1.0	0	117	57
		180	106 ± 0.5	0	189	133
		300	102 ± 1.5	0	235	181
		600	91.7 ± 1.8	0	296	246
		900	79.7 ± 7.9	1.68	315	262
		1800	55.7 ± 4.9	6.45	325	265
		2700	50.7 ± 8.3	6.31	326	263
	30	120	104 ± 7.9	0	256	149
		240	84.3 ± 8.2	1.26	356	241
		360	43.5 ± 3.7	6.21	475	286
		420	33.0 ± 8.1	6.87	490	291
		480	25.1 ± 3.4	8*	500	292
	50	60	106 ± 0.3	0	306	128
		90	98.2 ± 3.6	0.19	360	179
		100	96.2 ± 0.7	0.54	378	192
		120	80.3 ± 1.3	1.61	419	220
		140	69.5 ± 6.6	2.49	484	248
		160	58.1 ± 1.7	4.45	502	269

Note: Additionally, the ILSS (τ), delamination depth (z_d), front side temperature (T_{fs}), and back side temperature (T_{bs}) are listed.
Abbreviations: CFRPs, carbon fiber reinforced polymers; ILSS, interlaminar shear strength.
*When $z_d = z$, delaminations penetrate through the whole CFRP.

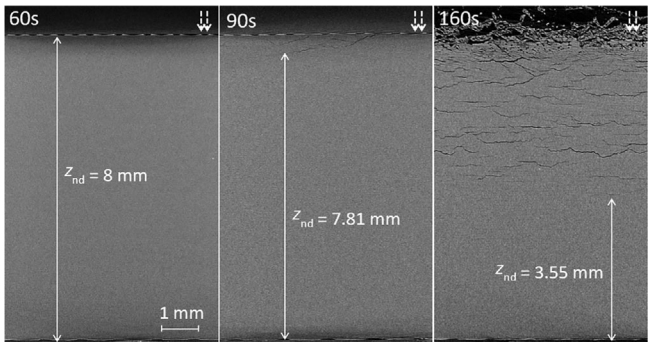

FIGURE 1 Three computed X-ray tomography-cross sections of carbon fiber reinforced polymers specimens irradiated at 50 kW/m^2 over different time intervals and with a thickness of 8 mm. The non-delaminated thickness z_{nd} is marked. Dotted arrows indicate the irradiated surface

plane with a defined step size between the measuring points resulting in a depth-resolution of 0.2 mm.

Delaminations were observed by means of the microfocused μCT system V-TOME XL 300 by GE Sensing & Inspection Technologies using a 300 kV microfocus X-ray source. For specimens with the dimension 8 mm × 8 mm × z mm, a resolution of 7.1 μm was obtained. The delamination depth z_d was determined by measuring the non-delaminated thickness z_{nd} (distance between deepest delamination and back side, see Figure 1) and subtracting it from the sample thickness z. An estimation of the uncertainty was about six voxels (= 42.6 μm) was expected.

ILSS testing was performed according to DIN EN 2563.[27] Thin specimens (z = 4 mm) have the dimensions 40 mm × 20 mm × 4 mm and were tested on a Zwick/Roell Z020. The distance between the supports was scaled up to 20 mm and the radii of the loading nose and supports to 5 mm. Thick specimens (z = 8 mm) were tested on a Zwick/Roell Zmart.Pro with specimen dimensions of 80 mm × 40 mm × 8 mm. Here, the distance of the supports was 40 mm and the radii of the loading nose and supports are 10 mm. Each mentioned ILSS τ is the mean of minimum three single values.

2.3 | Multivariate data analysis

Spectra for multivariate data analysis were pretreated by calculating the first derivative according to Savitzky–Golay (second polynomial order, 13 points) followed by standard normal variate transformation.[28] The relevant spectral range was limited from 1800 to 900 cm^{-1}. Data pretreatment as well as principal component analysis (PCA) and PLS regression were performed with the software The Unscrambler® X Version 10.5.1 by CAMO Software AS. Both PCA and PLS were performed with mean centered date. For both, seven principal components or factors respectively were calculated by using the Nipals algorithm.

For evaluating the quality of the models, two parameters were mainly used: The root mean square error of the calibration (RMSEC) and the coefficient of determination R^2, which describes the amount of the total variance of the dependent variable (ILSS, delamination depth) explained by the independent variables (spectral data). Furthermore, the explained variance and the BIAS, which is the mean of all residuals, were used for a further characterization of the model quality. Cross validation (CV) was calculated by leaving out randomly one object.[28]

3 | RESULTS AND DISCUSSION

3.1 | Degradation phenomena after one-sided thermal loading

3.1.1 | Structural damage and influence on residual strength

μCT is a well-accepted method to analyze structural damage inside CFRP. Figure 1 shows cross sections of CFRP samples with a thickness of 8 mm irradiated at 50 kW/m^2 for 60, 90, and 160 s. As shown in Figure 1, after an irradiation time of 90 s, delaminations occur near the irradiated surface. With further increasing irradiation time, delaminations penetrate deeper inside the CFRP as depicted for CFRP after thermal treatment for 160 s (also see Table 1). A characteristic parameter for structural damage inside the CFRP is the delamination depth z_d. Figure 2 shows the delamination depth for 4 and 8 mm thick specimens at different irradiation times irradiated at 50 kW/m^2. It is shown, that for thin specimens, delaminations migrate faster inside the CFRP than for thick ones, which is dominantly caused by the lower heat capacity and therefore higher temperatures occurring for thinner specimens.[29] For example, T_{fs} and T_{bs} for 4 mm thick CFRP irradiated for 60 s at 50 kW/m^2 were significantly higher than for 8 mm thick CFRP irradiated at the same heat flux and irradiation time (4 mm/8 mm: T_{fs} = 361°C/306°C, T_{bs} = 258°C/128°C; see Table 1). As the development of delaminations is inter alia dependent on temperature, structural damage occurs faster for thinner specimens.[18]

Furthermore, Figure 2 shows the ILSS for 4 and 8 mm thick specimens irradiated at 50 kW/m^2. Also, residual strength for thinner CFRP decreases faster than for thick CFRP. Comparing the courses of delamination

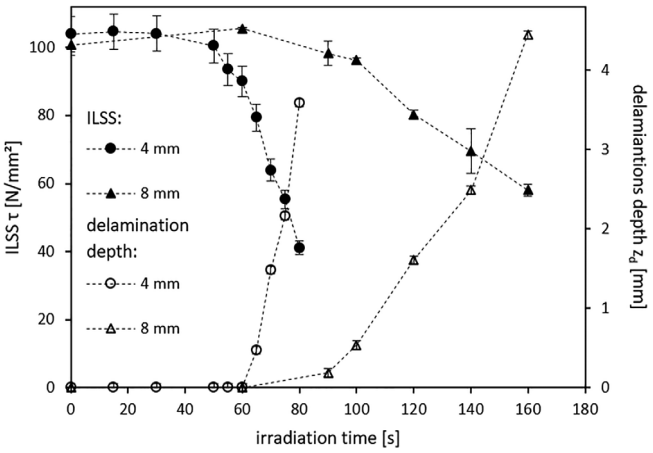

FIGURE 2 Interlaminar shear strength (ILSS) τ and the delamination depth z_d vs. the irradiation time for 4 and 8 mm thick carbon fiber reinforced polymers irradiated at 50 kW/m^2

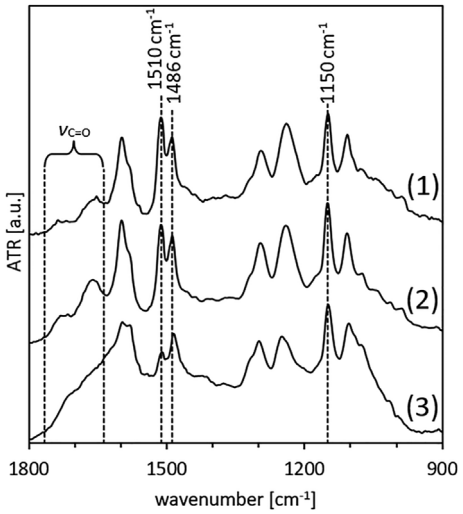

FIGURE 3 Attenuated total reflection Fourier transform infrared-spectra from the surface of 8 mm thick 8552/IM7 carbon fiber reinforced polymers specimens without thermal loading (1), after an irradiation at 50 kW/m^2 for 60 s (2) and 120 s (3)

depth and residual ILSS, ILSS noticeably decreases with increasing delamination depth. The same behavior can be observed for 4 and 8 mm thick specimens irradiated at 15 and 30 kW/m^2. For these lower heat fluxes, however, a longer irradiation time was necessary to induce delaminations and cause a loss in residual strength (see Table 1).[18]

3.1.2 | Matrix degradation

The irradiation-induced matrix degradation must also be taken into account to characterize thermal damage of CFRP. For this kind of damage, ATR-FTIR-spectroscopy is an appropriate detection method. Spectrum (1) in Figure 3 corresponds to the unloaded 8552/IM7. Besides epoxy resin, 8552/IM7 contains thermoplastic polyethersulfone (PES).[9] Both components can be found in the spectrum: the bands at 1510 and 1610 cm^{-1} correspond to the C—C stretching vibrations of the aromatic ring structure in the epoxy resin, whereas the bands at 1486 and 1586 cm^{-1} are characteristic for PES. Furthermore, the band at 1150 cm^{-1} can be assigned to the symmetric stretching vibration of the SO_2-group in PES.[6,30] The wavenumber range between 1650 and 1760 cm^{-1} can be assigned to C═O stretching vibrations of oxidized surface species. Figure 3 depicts spectra of surfaces of CFRP after thermal treatment at 50 kW/m^2 for 60 and 120 s. It can be shown, that broad bands between 1650 and 1760 cm^{-1} arise with increasing thermal loading due to the presence of oxygen on the surface which, in combination with temperature, causes thermo-oxidative degradation of the epoxy resin.[31,32] Due to the limited diffusion of oxygen into the CFRP, this thermo-oxidative reaction occurs only close to the irradiated surface (max. penetration depth ~100 µm).[33] Furthermore, with increasing thermal loading, the intensity of the 1510 cm^{-1} band, which is characteristic for the less thermally stable epoxy resin, decreases while the band for the more stable PES at 1486 cm^{-1} remains constant. Therefore, the intensity ratio of the bands at 1510 and 1486 cm^{-1} is characteristic of matrix degradation caused by thermal loading and can be denoted as a damage quantity.[9]

This ratio is calculated from spectra measured along a ground incline plane to generate depth profiles of matrix degradation for one-sided thermally treated CFRP. Figure 4 shows depth profiles for CFRP with a thickness of 8 mm irradiated at 50 kW/m^2 for (A) 60, (B) 120, and (C) 160 s, respectively. In the early stage of irradiation (60 s), no matrix degradation can be observed in the specimens. A decrease of $I_{1510\ cm^{-1}}/I_{1486\ cm^{-1}}$ can be recognized close to the irradiated surface (0 mm) for specimens irradiated for 120 s. After 160 s, the specimen surface was strongly damaged and a gradient of matrix degradation through the CFRP was clearly visible.

Additionally, the delamination depth measured with µCT is marked by vertical dotted lines. These lines cross the gradients of matrix degradation at a value of ~0.71 for $I_{1510\ cm}$-1/$I_{1486\ cm}$-1 for 120 and 160 s. This value corresponds to the calculated threshold value of 0.74 ± 0.05, below which the formation of delaminations in 8552/IM7 occurs.[18] The threshold value is indicated by the horizontal line in Figure 4. Interestingly, the horizontal and vertical lines cross where the drop of the $I_{1510\ cm}$-1/$I_{1486\ cm}$-1 curves start when approaching the front side of the sample. It is concluded, that above these depths,

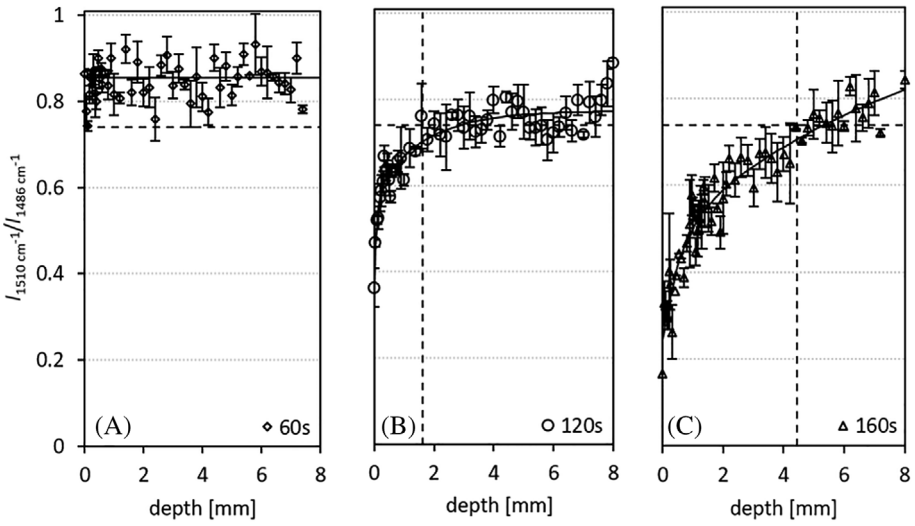

FIGURE 4 Intensity ratio of the bands at 1510 and 1486 cm^{-1} plotted against the sample depth of 8 mm thick carbon fiber reinforced polymers (0 mm = irradiated surface) irradiated at 50 kW/m^2 for (A) 60 s, (B) 120 s and (C) 160 s. The horizontal dotted line indicates the threshold value of matrix degradation, below whose delaminations develop[17]; the vertical dotted lines mark the delamination depth measured with computed X-ray tomography

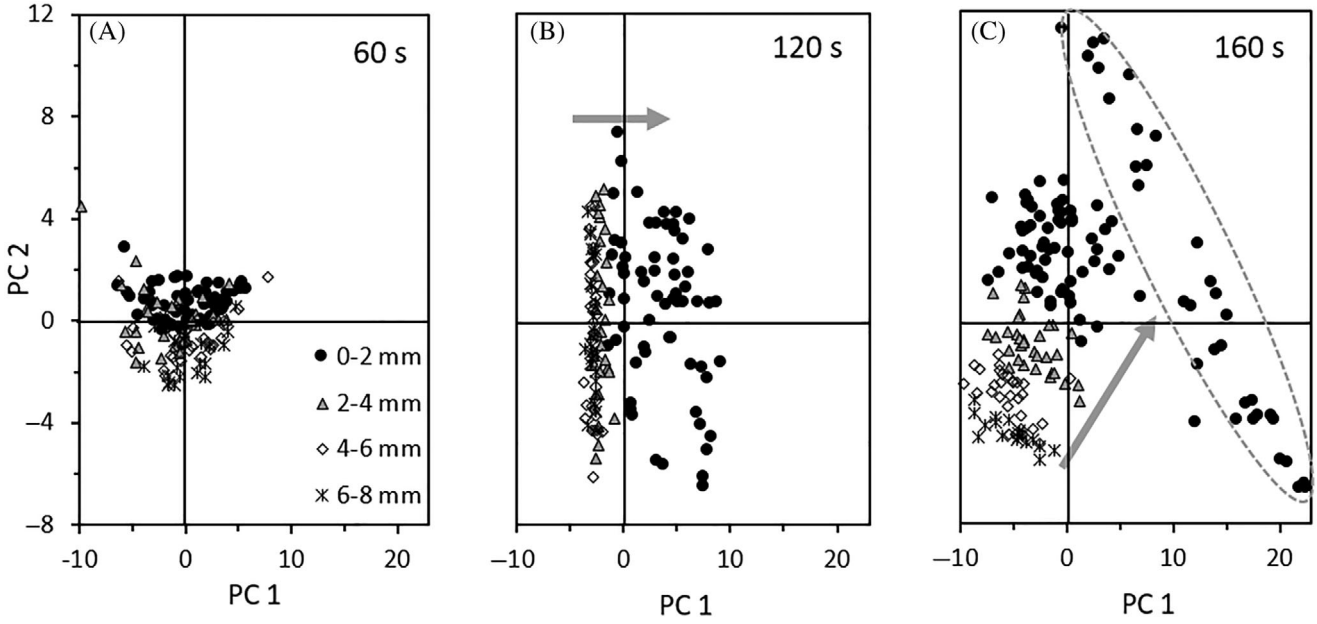

FIGURE 5 Score plot of a principal component analysis calculated by using spectra of different depths of 8 mm thick carbon fiber reinforced polymers samples irradiated at 50 kW/m^2 for (A) 60 s, (B) 120 s, and (C) 160 s (arrows mark increasing thermal damage; dotted ellipse marks strong thermal damage between 0 and 0.7 mm with exposed fiber-bundles). The data points are assigned to four different depth ranges

delaminations are responsible for reduced heat conduction toward the back side of the sample and cause pronounced matrix degradation.[34]

3.2 | PCA of IR spectra

The application of multivariate data analysis in the form of PCA allows for the exploration of spectral data (FTIR) patterns.[28,35] In a PCA, multidimensional data like, for example, spectra from different samples are reduced to fewer dimensions by calculating new latent variables called principal components (PCs) or factors. They are the axes of a new coordinate system displaying the maximum variance in the spectral data. A score plot shows the samples transferred as scores into the new coordinate system. The measure of how strong single variables (e.g. wavenumbers of spectra) influence the position of a score in the PC coordinate system can be seen in a loading plot. A detailed description of the calculation of a PCA can be found in ref. [28].

PCA was applied on the depth-resolved spectral data belonging to 8 mm thick CFRP specimens irradiated for 60, 120, and 160 s at 50 kW/m^2 as shown in Figure 4. The

resulting score plots for PC 1 and PC 2 are shown in Figure 5. The data points were organized in four groups belonging to different depth ranges inside the specimens (0–2 mm, 2–4 mm, 4–6 mm, and 6–8 mm). For the spectra taken after 60 s of irradiation, the score plot shows data points lying close together. After an irradiation of 120 s, data points were more spread out (see Figure 5(B)). It is noticeable that the data points with a sample depth between 2 and 8 mm lie close together, whereas only the data points in the range of 0–2 mm (black dots in Figure 5(B)) were separated. Regarding Figure 4(B), in this depth range pronounced matrix degradation and delaminations were observed, whereas thermal degradation was not pronounced between 2 and 8 mm. The loadings, which mainly influence and separate the scores along PC 1 and thus regarding thermal loading, are dominated by the wavenumbers around 1510 cm^{-1} (negative load on PC 1) for intact CFRP and around 1150 and 1486 cm^{-1} (positive load on PC 1) for thermally damaged CFRP. Therefore, it is shown that PCA separates data regarding thermal damage and according to Section 3.1.2, where these two bands are discussed to be characteristic for thermal loading.

The score plot for CFRP treated at 160 s in Figure 5 (C) shows an even more pronounced separation of the data. The data points corresponding to spectra indicating strong matrix degradation and delaminations (0–4 mm, black dots and gray triangles) were most separated. The data are distributed along PC 1 according to the separation at 120 s. Further, a strong separation of the data points is recognized along PC 2 for samples taken in a depth range between 0 and 0.7 mm (see ellipse in Figure 5(C)), where thermal degradation of the matrix already leads to the exposure of fiber bundles.

In summary, it is shown that the application of PCA allows the separation of spectral data regarding thermal loading, where strongly delaminated and non-delaminated areas of the CFRP can be identified. Considering the influence of delaminations on residual strength (see Section 3.1.1), the use of infrared spectroscopy in combination with multivariate data analysis should allow the prediction of residual strength.

3.3 | Prediction of the residual ILSS using multivariate data analysis

Due to the sensitivity of the IR spectra regarding thermally induced structural damage (see Section 3.1.2), the IR spectra can be used for the prediction of mechanical properties (ILSS) and structural damage (delamination depth). PLS regression proved to be an appropriate multivariate calibration tool.[10,21–24] For PLS, separate PCAs of spectral and response (e.g. ILSS) data are calculated while simultaneously maximizing the covariance between those data. The calculated loadings can be used to create a linear regression equation. The response parameter of an unknown sample can be predicted with this equation by using spectral data. A detailed description of the calculation of a PLS can be found in ref. [28].

In the following chapters, different PLS models are shown and discussed with view on their prediction quality. With the aim of finding a preferably universally applicable PLS model, models were built for different parameter settings (PS). Therefore, four groups of data with different parameter settings are introduced (see Table 2): The simplest PS-1 contains spectra of CFRP with a thickness of 8 mm irradiated at 50 kW/m^2. This parameter setting mainly serves as reference because only one heat flux and one specimen thickness are considered. To investigate the influence of the heat flux, PS-2 is introduced containing 8 mm thick CFRP irradiated at 15, 30, and 50 kW/m^2. PS-3 includes 4 and 8 mm thick specimens irradiated at 50 kW/m^2 and was used for observing the influence of varying sample thickness. Finally, PS-4 involves the whole data set, i.e. 4 and 8 mm thick CFRP irradiated at 15, 30, and 50 kW/m^2. All abbreviations as well as the corresponding RMSECV and R^2 (Cross Validation) of the different models are listed in Table 2 for the prediction of both ILSS and the standardized delamination depth z_d/z.

3.3.1 | PLS with spectra taken at the surface of the CFRP

First, spectra for modeling were taken at the irradiated surface of 8 mm thick CFRP specimens after thermal loading at 50 kW/m^2 for different time intervals (PS-1). Figure 6(A) contrasts the calculated and the measured ILSS. The PLS model shows an RMSEC of 0.4 N/mm^2 and a corresponding R^2 of 0.999 as well as an RMSECV of 2.1 N/mm^2 and a corresponding R^2 of 0.987. Thus, a good prediction quality can be achieved for CFRP with one thickness irradiated at one heat flux. With increasing complexity of the sample parameters (PS-1 → PS-2/PS-3 → PS-4), the RMSE increases and R^2 decreases. Varying only one parameter, i.e. adding either a sample thickness or additional heat fluxes downgrade the prediction quality (see Table 2), the deterioration is approximately similar for PS-2 and PS-3 (PS-2 RMSECV: 8.3 N/mm^2; PS-3 RMSECV: 8.5 N/mm^2). The maximum variation of sample parameters regarded in this work includes CFRP irradiated at 15, 30, and 50 kW/m^2 for different irradiation times and with thicknesses of 4 and 8 mm (PS-4), i.e. both sample thickness and heat flux are varied. ILSS

TABLE 2 Overview over the sample parameters used for generating different PLS models with the resulting RMSECV and R^2 (cross validation) values for each model

Parameter setting (PS)	Sample thickness, heat flux	Number of combined spectra	Depth of taken spectra (mm)	Size dataset (objects × variables)	RMSECVILSS (N/mm²)	R^2ILSS	RMSECVz_d/z(−)	R^2z_d/z
PS-1	8 mm, 50 kW/m²	1	0/−/−/−	21 × 468	2.1	0.987	0.05	0.925
			bs*/−/−/−	21 × 468	5.3	0.908	0.05	0.941
		2	0/0.2/−/−	28 × 936	1.0	0.998	0.03	0.979
			0/bs*/−/−	32 × 936	1.5	0.994	0.02	0.992
		3	0/0.2/0.4/−	48 × 1404	0.5	0.999	0.01	0.999
		4	0/0.2/0.4/0.6	459 × 1872	0.5	0.999	0.01	0.999
PS-2	8 mm,15, 30 and 50 kW/m²	1	0/−/−/−	38 × 468	8.3	0.872	0.10	0.869
			bs*/−/−/−	42 × 468	9.7	0.836	0.14	0.787
		2	0/0.2/−/−	53 × 936	3.6	0.976	0.04	0.982
			0/bs*/−/−	100 × 936	4.3	0.961	0.06	0.964
		3	0/0.2/0.4/−	86 × 1404	2.5	0.987	0.04	0.975
		4	0/0.2/0.4/0.6	583 × 1872	1.3	0.995	0.02	0.996
PS-3	4 and 8 mm,50 kW/m²	1	0/−/−/−	48 × 468	8.5	0.852	0.16	0.817
			bs*/−/−/−	50 × 468	5.5	0.942	0.07	0.945
		2	0/0.2/−/−	119 × 936	5.5	0.959	0.10	0.929
			0/bs*/−/−	129 × 936	2.9	0.986	0.06	0.969
		3	0/0.2/0.4/−	96 × 1404	2.8	0.980	0.05	0.970
		4	0/0.2/0.4/0.6	1029 × 1872	2.6	0.987	0.04	0.975
PS-4	4 and 8 mm,15, 30 and 50 kW/m²	1	0/−/−/−	83 × 468	9.9	0.833	0.17	0.786
			1/−/−/−	70 × 468	7.2	0.910	0.10	0.907
			2/−/−/−	68 × 468	9.1	0.863	0.18	0.755
			3/−/−/−	69 × 468	10.4	0.827	0.17	0.741
			bs*/−/−/−	92 × 468	9.8	0.837	0.15	0.843
		2	0/0.2/−/−	215 × 936	5.8	0.948	0.11	0.922
			1/1.2/−/−	153 × 936	4.8	0.964	0.08	0.949
			2/2.2/−/−	142 × 936	6.5	0.938	0.11	0.910
			3/3.2/−/−	193 × 936	7.4	0.906	0.13	0.862
			0/1/−/−	192 × 936	5.5	0.946	0.11	0.940
			0/2/−/−	178 × 936	5.8	0.946	0.13	0.885
			0/bs*/−/−	274 × 936	6.3	0.931	0.11	0.916

(Continues)

TABLE 2 (Continued)

Parameter setting (PS)	Sample thickness, heat flux	Number of combined spectra	Depth of taken spectra (mm)	Size dataset (objects × variables)	RMSECVILSS (N/mm^2)	R^2ILSS	RMSECVz_d/z(–)	R^2z_d/z
		3	0/0.2/0.4/–	214 × 1404	4.8	0.959	0.09	
			1/1.2/1.4/–	218 × 1404	3.6	0.979	0.06	0.973
			2/2.2/2.4/–	206 × 1404	4.6	0.967	0.08	0.946
			3/3.2/3.4/–	198 × 1404	4.3	0.971	0.08	0.956
			0/1/2/–	440 × 1404	3.8	0.976	0.06	0.968
			0/2/4/–	608 × 1404	4.3	0.971	0.08	0.957
		4	0/0.2/0.4/0.6	1297 × 1872	3.8	0.973	0.08	0.941
			1/1.2/1.4/1.6	608 × 1872	3.6	0.977	0.06	0.973
			2/2.2/2.4/2.6	506 × 1872	4.5	0.972	0.08	0.957
			3/3.2/3.4/3.6	603 × 1872	3.7	0.978	0.06	0.971
			0/1/2/3	1328 × 1872	4.1	0.970	0.07	0.954

Abbreviations: ILSS, interlaminar shear strength, PLS, partial least squares regression; RMSECV, root mean square error cross validation.
*bs = back side = 4 or 8 mm; 0 mm = irradiated surface; objects = number of spectra, variables = wavenumbers.

calculated with this PLS model is shown in Figure 6(B). An R^2 (calibration) of 0.916 and an RMSEC of 7 N/mm^2 a as well as an R^2 (CV) of 0.833 and an RMSECV of 9.9 N/mm^2, which corresponds to an error of about 10%, were obtained. As the RMSE and R^2 for the calibration are optimistic because spectra are used simultaneously for calculating the model and RMSE and R^2, in the following chapters, RMSE and R^2 only for cross validation are used for getting a more realistic assessment of the models.

Further, the standardized delamination depth z_d/z was predicted by using surface spectra. R^2 for the prediction of the delamination depth (see Table 2) decreased from 0.925 for PS-1 over 0.869 (PS-2) and 0.817 (PS-3) down to 0.786 for PS-4. Here, the variation of the sample thickness (PS-3) led to a more pronounced deterioration of the prediction quality than the variation of the heat flux (PS-2). Analogously, the RMSECV increased from 0.05 (PS-1) to 0.17 (PS-4), which is an error of 17%. Comparing the RMSECV and R^2 for the prediction of the delamination depth and ILSS, PLS models predicting ILSS show a better prediction quality than models predicting the delamination depth. An explanation for this can be the detection limit of the µCT due to the maximum resolution of 7.1 µm for detecting all delaminations. This means that smallest delaminations are not detected and therefore structural damage cannot be considered thoroughly. However, ILSS can be affected by a thermally induced weakening of the fiber-matrix-adhesion and therefore displays structural thermal damage more globally.

Additionally, PLS models were established by using single back side spectra (see Table 2). It is shown, for example, that the RMSECV of a PLS model established with CFRP specimens with PS-4 is 9.8 when using back side spectra and 9.9 when using spectra from the irradiated surface. Despite a better spectra quality of the back side spectra due to not exposed fiber bundles at the surface, no improvement in the prediction quality was achieved. This lack of improvement can be explained by the lower variance of the spectral data concerning thermal loading at the back side of the CFRP (see Figure 4).

Summarizing, it is shown, that with increasing complexity of the parameter settings, the prediction quality decreases for models built with single surface spectra, which is why this model should only be used for one sample thickness and one heat flux to get a reliable prediction.

3.3.2 | Combination of spectra taken at the front and back side of the CFRP

A possible way to improve the prediction quality is to take spectra at different depths of the CFRP and combine

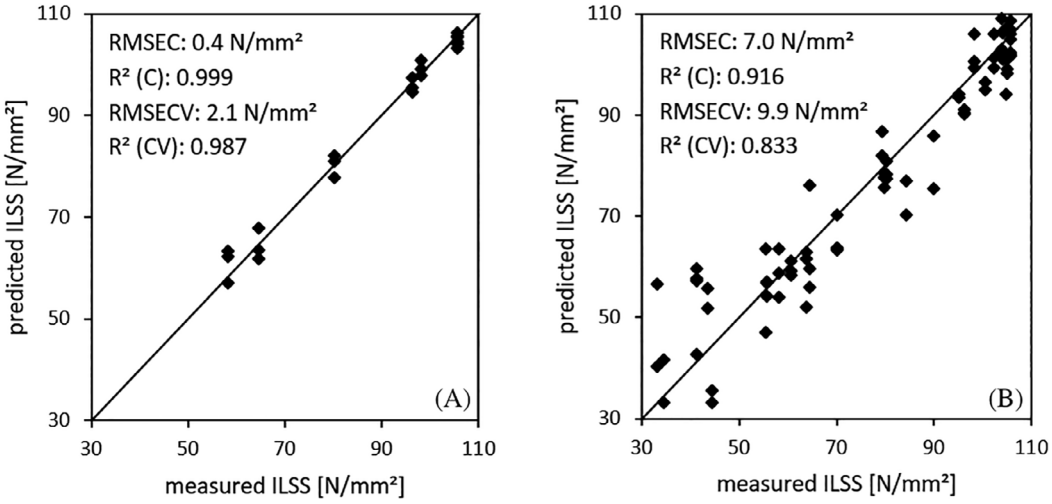

FIGURE 6 Measured vs. predicted interlaminar shear strength values determined with partial least squares-models using IR spectra taken at the irradiated surface of: (A) 8 mm thick CFRP samples treated at 50 kW/m^2 (PS-1) 0(B) 4 and 8 mm thick CFRP after an irradiation at 15, 30, and 50 kW/m^2 (PS-4) (calibration data are depicted, RMSE and R^2 are given for calibration (C) and cross validation [CV]). CFRPs, carbon fiber reinforced polymers; PS, parameter setting; RMSE, root mean square error

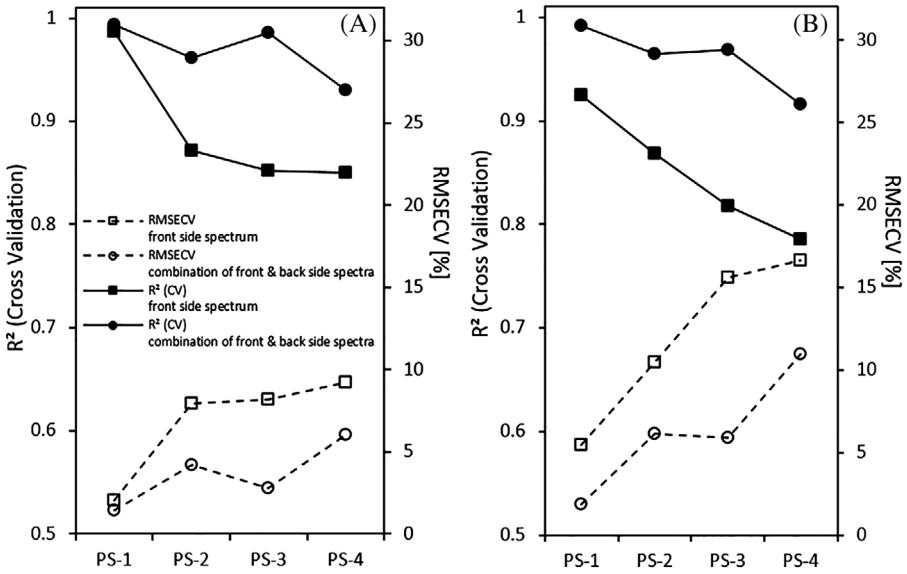

FIGURE 7 R^2 and root mean square error cross validation of partial least squares models built by only taking the irradiated surface spectra and by combining spectra taken at the irradiated surface and the back side of carbon fiber reinforced polymers with different parameter settings for the prediction of interlaminar shear strength (A) and the depth of delaminations (B) (PS-1 to PS-4: see Table 2). PS, parameter setting

them for PLS to predict ILSS and delamination depth. The simplest way to accomplish this would be to combine the front and back side spectra. R^2 and RMSECV for the PLS models built for PS-1 to PS-4 are depicted in Figure 7. It is shown that the combination of front and back side spectra leads to a better prediction quality compared with models just using single surface spectra for the prediction of both ILSS and delamination depth. For example, the RMSECV for the predicted ILSS or delamination depth z_d/z for PS-4 decreases from 9.9 or 0.17 for PLS models taking only the surface spectra into account and to 6.3 or 0.11, respectively, for PLS models considering front and back side spectra. Furthermore, the prediction quality decreases less with increasing complexity of parameter settings for the models using combined spectra than for those using single spectra. Also, models predicting ILSS show a better prediction quality (lower RMSECV and higher R^2) than models predicting the delamination depth due to more thorough consideration of structural damage by ILSS (see Section 3.3.1). However, it is noticeable, that the prediction quality for the parameter setting PS-3 is especially lower for the prediction of ILSS than for PS-2, i.e. models established by combining spectra from two sides lose more prediction quality with increasing variation of heat flux than of sample thickness.

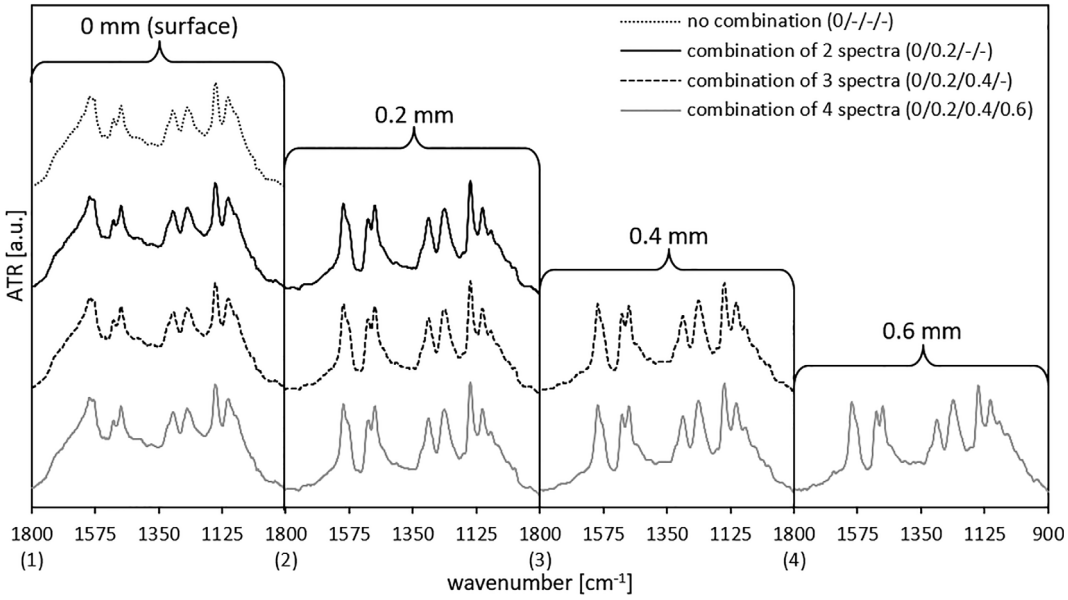

FIGURE 8 Illustration of the combination of spectra taken in different depths exemplarily shown for 8 mm thick carbon fiber reinforced polymers irradiated for 120 s at 50 kW/m^2

3.3.3 | Combination of spectra taken at different depths close to the irradiated surface of the CFRP

Due to the improvement of the prediction quality by combining front and back side spectra, a further way to enhance the prediction quality is to combine spectra from different depths, i.e. spectra taken not only at the surface but also taken inside the CFRP. Due to the combination of spectra from different depths to predict ILSS and delamination depth by PLS, inhomogenously distributed thermal damage inside the CFRP (see Figure 4) can be incorporated in the model. Therefore, CFRP layers with a defined thickness Δz have to be removed mechanically, e.g. by grinding or milling. A constant Δz of 0.2 mm is chosen. A first spectrum was recorded at the irradiated surface. After the first grinding process, the next spectrum was taken 0.2 mm deeper and so on down to the deepest required spectrum (dependent on the total number of combined spectra). The recorded spectra were pretreated separately and subsequently combined by stringing them together. Figure 8 shows the juxtaposition of spectra and the different strong pronounced matrix degradation dependent on the sample depth. Regarding the intensities for the band at 1510 cm^{-1}, which is characteristic for the less thermally stable epoxy resin, it can be seen that spectra taken in deeper areas of the specimen show a higher intensity (cf. Figure 4).

The calculation of a predicted value (e.g. ILSS τ) with a PLS model using spectra taken at different depths was done according to the following regression Equation (1). The spectral intensities I were strung together and multiplied with the regression coefficients b. In (1), i is the number of the spectrum (i_{max} = number of combined spectra), j is the number of the variable in the respective spectrum, and b_0 is a constant value, which is defined together with the regression coefficients in the calibration of the model.

$$\tau = b_0 + \left[I_{1,1}\, I_{1,2} \cdots I_{2,1}\, I_{2,2} \cdots I_{i,j}\right] \cdot \left[b_{1,1}\, b_{1,2} \cdots b_{2,1}\, b_{2,2} \cdots b_{i,j}\right]^T \quad (1)$$

Below, RMSECV and R^2 are discussed for PLS models established with a varying number of combined spectra and for different parameter settings. Figure 9(A) shows the R^2 and RMSECV for the calibrated PLS model for predicting ILSS. For PS-1, all PLS models show good prediction quality due to no variation in the sample parameters. With increasing complexity of the parameter settings (from PS-1 to PS-4), RMSECV increases and R^2 decreases for the PLS model built with one spectrum (see Section 3.3.1). For PLS models established with two combined spectra with a distance of 0.2 mm, however, a decrease for the RMSECV of about 40% was observed for PS-4 compared with the RMSECV calculated with the PLS done with single surface spectra. With increasing number of combined spectra, the RMSECV value further decreases about 50% for four combined spectra (see also Table 2).

Regarding the prediction of the delamination depth with combined spectra (see Figure 9(B)), an improvement

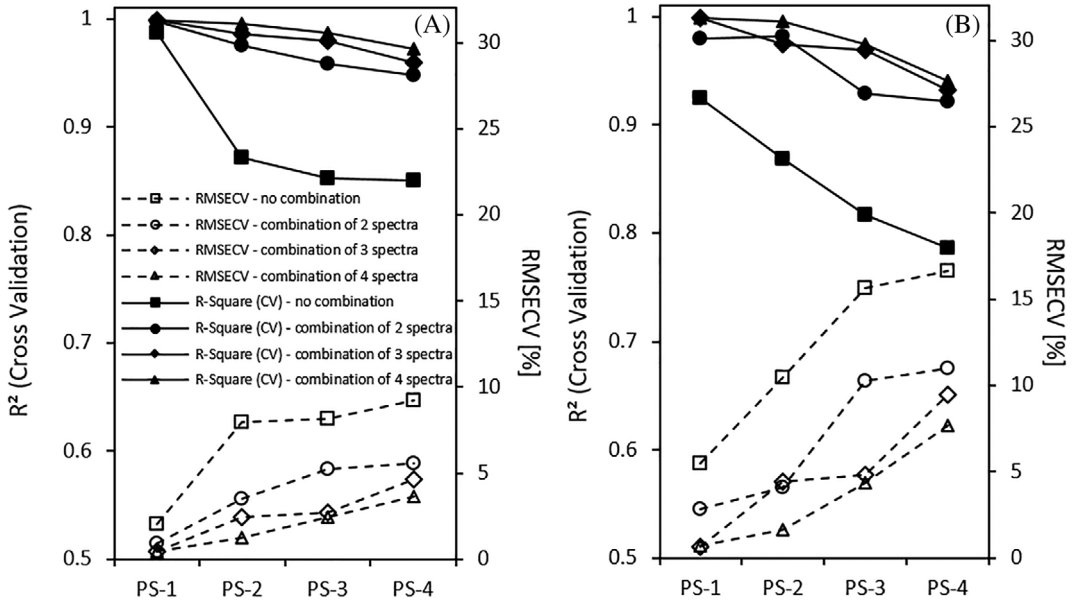

FIGURE 9 R^2 and root mean square error cross validation of partial least squares-models built by combining no, 2, 3, or 4 spectra taken in different depths with a constant step size of 0.2 mm starting at the irradiated surface of carbon fiber reinforced polymers with different parameter settings for the prediction of interlaminar shear strength (A) and the depth of delamination (B) (PS-1 to PS-4: see Table 2)

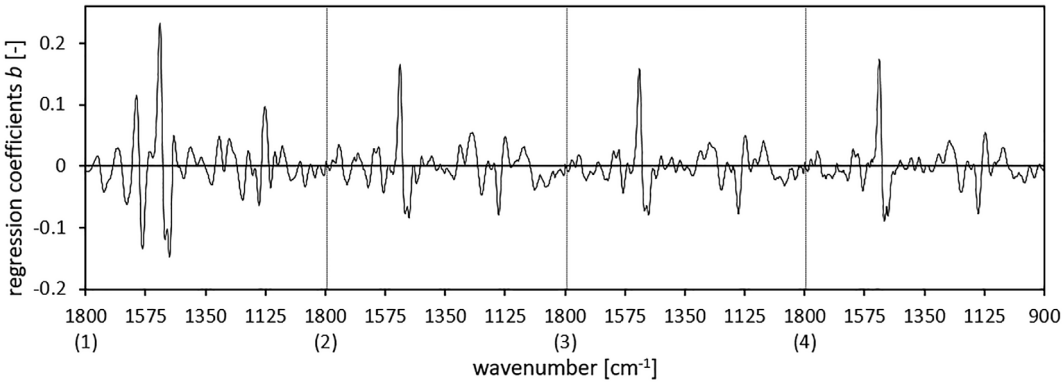

FIGURE 10 Regression coefficients for factor one of the partial least squares-model with four combined spectra taken at the irradiated surface and in the depths 0.2, 0.4, and 0.6 mm of PS-4 carbon fiber reinforced polymers samples used for the prediction of the residual interlaminar shear strength

of the prediction quality can also be achieved with an increasing number of combined spectra. But as already mentioned for the PLS models established by using single surface spectra, models for the prediction of ILSS show a better prediction quality than models predicting the delamination depth due to limited resolution of the µCT (see Section 3.3.1). Therefore, in the following discussion, the focus lies on the prediction of ILSS.

The regression coefficients, *b*, give insight as to how strong the predicted value is influenced by different spectral regions. Analyzing the regression coefficients of the PLS model can help to understand why ILSS can be predicted by using IR spectra and why the prediction quality can be increased by combining spectra. Figure 10 depicts the regression coefficients for the PLS model created by combining four spectra for PS-4. It is shown that the regression coefficients especially around 1525 cm^{-1} (wavenumber after pretreatment, corresponds to the band at 1510 cm^{-1}) show a high influence. As discussed for Figure 3 (Section 3.1.2), the band at 1510 cm^{-1} decreases with increasing thermal loading. This means that if there is a high intensity at 1510 cm^{-1}, which is accompanied by no or low thermal loading, a high ILSS value is calculated due to the strong influence of this spectral region on the calculation of the ILSS. In contrast, for a low intensity at 1510 cm^{-1} associated with strong thermal damage, subsequently a lower ILSS value is calculated. Furthermore, the high influence of the bands at

TABLE 3 Explained variance and bias for each factor of the PLS-model built by combining spectral data taken at the irradiated surface and in different depths with a step size of 0.2 mm of CFRP (PS-4) for the prediction of the residual ILSS (comb. = combination)

	Explained variance (%)				Bias			
	No comb.	Comb. of two spectra	Comb. of three spectra	Comb. of four spectra	No comb.	Comb. of two spectra	Comb. of three spectra	Comb. of four spectra
Factor 1	68.1	73.2	65.5	74.7	0.58	0.10	0.01	0.02
Factor 2	71.0	87.4	77.8	82.0	0.09	−0.21	0.01	0.00
Factor 3	79.6	91.0	87.4	87.7	−0.09	0.24	−0.03	0.00
Factor 4	83.4	92.8	90.5	92.9	−0.16	−0.01	−0.01	0.00
Factor 5	85.8	94.6	94.7	95.6	0.87	−0.02	0.00	0.00
Factor 6	90.0	95.5	95.6	96.9	−0.06	0.01	0.08	0.01
Factor 7	91.6	96.6	96.8	97.4	0.04	0.06	0.15	0.02

Abbreviations: CFRPs, carbon fiber reinforced polymers; ILSS, interlaminar shear strength.

1510 cm^{-1} is given for all four combined spectra. This means that spectra from different depths corresponding to different strong thermal damage are used and therefore the inhomogenous distribution of thermal damage inside the CFRP (see Figure 8) is considered for calculating the ILSS. Having the highest regression coefficients for the spectral area around 1525 cm^{-1} is also ascertained for the combination of two or three spectra. But as shown in Figure 9, with increasing number of combined spectra, a better prediction quality can be achieved, which can be explained by the consideration of the thermal loading at four different depths and therefore the best reproduction of the inhomogenously distributed thermal damage. Furthermore, the stronger influence of the regression coefficients for the spectra of the irradiated surface (spectrum 1) compared to the ones of the other spectra taken in deeper areas can be assigned to additional thermo-oxidative degradation. This degradation occurs due to the oxidative atmosphere at the surface, which leads to a more pronounced matrix degradation than in the absence of oxygen (see Section 3.1.2).[7] The thermo-oxidation can also be seen at the more pronounced signals around 1650 cm^{-1} for the surface spectrum (1) compared with spectra (2) to (4) in Figure 10.

Additionally, further parameters for assessing the prediction quality were considered. The explained variance (see Table 3) provides information about how much of the variance of the ILSS can be explained per factor, i.e. the higher the explained variance the better. It is shown that the explained variance for PLS models with combined spectra is higher than for the PLS model using only single surface spectra. The models with combined spectra no longer show any increase of the explained variance from factor five, while the explained variance of the model with the single surface spectra increases up to a factor of seven. Consequently, models with combined spectra need less factors to describe the variance than a model solely based on single surface spectra.

Furthermore, the bias is regarded, which is defined as the mean of all residuals (difference between predicted ILSS and measured ILSS). In general, for a good calibration, the bias lies very close to zero. Table 3 further presents the bias for all factors of PLS models with varying numbers of combined spectra. It is shown that the bias for the model with no combined spectra is notably higher compared to the models with combined spectra. Furthermore, with increasing number of combined spectra, the bias lies closer to zero, which shows that the combination of more spectra leads to a better calibration. The unusually high bias for factor six and seven of the models with three and four combined spectra can be explained by increasing consideration of the spectral noise and not important spectral information anymore in the model, i.e. the best prediction of ILSS by using three or four combined spectra can be achieved by using five factors.

Finally, it was investigated whether the improvement of the prediction quality results only from the combination of any multiple spectra and therefore from an expanded data set or by combining spectral data at different depths. Therefore, different PLS models were established using different measured spectra at only one depth (irradiated surface [0 mm]). Additionally, one measured spectrum was strung together several times and a mathematically calculated random noise (sum of the spectral intensity ±10% of the intensity) was added to each spectrum. Table 4 shows both RMSECV and R^2 for PLS models of spectra taken at the irradiated surface of CFRP specimens (PS-4) with varying number of combinations. Despite increasing number of combined spectra, no significant improvement in the prediction quality was achieved. Therefore, a sole combination of spectra does not enhance the prediction quality. This

TABLE 4 RMSECV and R^2 of PLS models using various numbers of combined spectra from the irradiated surface established for CFRP (PS-4) to predict ILSS

Number of combined spectra	Depth of taken spectra [mm]	Type of spectra	RMSECV ILSS [N/mm²]	R^2 ILSS
1	0/−/−/−	measured	9.9	0.833
2	0/0/−/−	measured	9.1	0.865
	0/0/−/−	random noise	9.8	0.845
3	0/0/0/−	measured	12.0	0.749
	0/0/0/−	random noise	9.0	0.867
4	0/0/0/0	random noise	9.3	0.855

Note: The combined spectra are either measured at different spots on the surface or a random noise is added mathematically.
Abbreviations: CFRPs, carbon fiber reinforced polymers; ILSS, interlaminar shear strength; RMSECV, root mean square error cross validation.

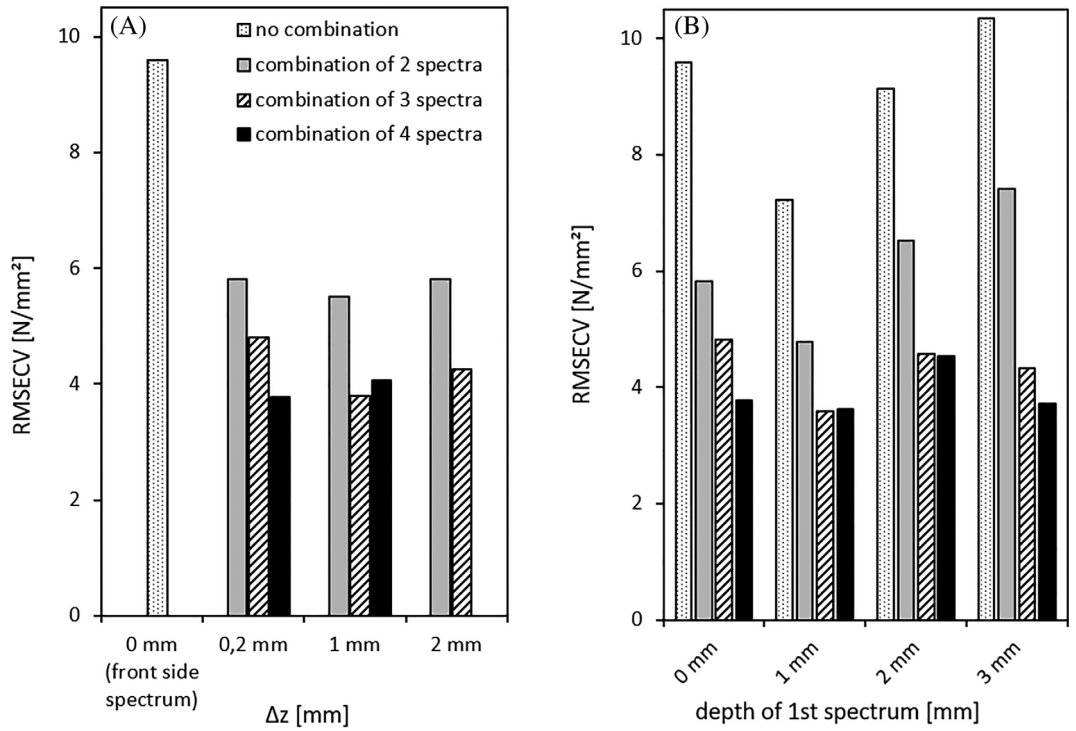

FIGURE 11 Root mean square error cross validation of partial least squares models for the prediction of interlaminar shear strength built by taking one spectrum or combining 2, 3, or 4 spectra taken (A) in different depths with a varying step size Δz starting at the irradiated surface and (B) in varying depth but with a constant step size between the spectra of 0.2 mm of PS-4 carbon fiber reinforced polymers

improvement results from the combination of spectra taken at different depths and the accompanying improved consideration of the inhomogeneously distributed thermal damage inside the specimens.

3.3.4 | Influence of the depth of the combined spectra on the prediction quality

Due to the inhomogenously distributed thermal damage inside the CFRP, the influence of the depth, where the spectra were recorded, as well as the step size into the depth between the combined spectra was investigated. Table 2 lists all RMSECV and R^2 for the prediction of ILSS and the standardized delamination depth. In the following section, the prediction of ILSS of PS-4 CFRP specimens will be discussed. For the influence of step size and depth of recorded spectra on the prediction of the delamination depth, a comparable behavior was found (see Table 2).

At first, the step size between the spectra was varied. Figure 11(A) shows the RMSECV for PLS models

TABLE 5 RMSECV and R^2 of PLS models using various numbers of combined spectra taken in different depths with a step size of $\Delta z = 0.2$ mm for only one specific depth (first spectrum taken at 0 mm) or for different depth ranges established for CFRP (PS-4) to predict ILSS

	No combination		Combination of two spectra		Combination of three spectra	
	RMSECV (N/mm^2)	R^2	RMSECV (N/mm^2)	R^2	RMSECV (N/mm^2)	R^2
0 mm	9.93	0.833	5.82	0.948	4.81	0.959
0 to 0.6 mm	9.19	0.833	7.17	0.916	6.24	0.931
0 to 1 mm	9.39	0.826	7.22	0.912	6.55	0.925
0 to 2 mm	10.50	0.792	8.24	0.887	8.03	0.891

Abbreviations: CFRPs, carbon fiber reinforced polymers; ILSS, interlaminar shear strength; PLS, partial least squares; RMSECV, root mean square error cross validation.

established by combining different numbers of spectra for three different step sizes Δz (0.2, 1.0, and 2.0 mm) into the depth starting with the spectrum at $z = 0$ mm. This means, for example, that spectra were taken at a depth of 0, 1, and 2 mm for the combination of three spectra with $\Delta z = 1.0$ mm. As expected, the RMSECV decreases with increasing number of combined spectra. However, no trend was apparent for increasing step size, i.e. for a constant Δz between the spectra, the distance between the gathered spectra seems to be secondary. This can be explained by two contrary effects: small Δz are more sensitive toward thermal loading due to the steeper slope occurring close to the irradiated surface. Conversely, bigger Δz values are more representative for the total damage distribution inside the specimens. Due to no apparent trend for changing step sizes, it seems that both explanations can be weighted equally. Consequently, for practical application, Δz should be chosen as small as possible to avoid the mechanical removal of a high amount of CFRP, which reduces the sample thickness and therefore causes a higher effort to repair.

Furthermore, the depth at which the spectra were taken was varied. Spectra are taken with a constant distance Δz into depth of 0.2 mm (see Section 3.3.3) but at different depths z of 0, 1, 2, and 3 mm. This means, for example, that spectra for a combination of three spectra at a depth of 1 mm were taken at 1, 1.2, and 1.4 mm. Figure 11(B) shows the RMSECV for PLS models established for single spectra and for combined spectra of a maximum of four spectra at different depths for the prediction of ILSS. Using single spectra from the irradiated surface (no combination), a high RMSECV was observed for the PLS model using surface spectra. The PLS model based on single spectra taken at a depth of 1 mm shows a lower RMSECV. Compared with the surface model, different pronounced thermal damage can still be observed at 1 mm but with the advantage of not having free fiber-bundles on the sample surface after strong thermal loading, which deteriorate the spectra quality and therefore the prediction quality of a model. Furthermore, the RMSECV increased again with increasing depth because spectra at deeper areas of the CFRP showed less variation regarding thermal loading due to lower thermal damage occurring deeper inside the CFRP (see Figure 4). It is shown, that for increasing number of combined spectra, the RMSECV decreases. In addition, the differences between the RMSECV values at different depths for each number of combinations decrease for increasing number of combined spectra. This means that with higher numbers of combined spectra, influences caused by the depth at which the spectra were taken can be reduced.

Finally, the manner in which spectra are gathered at specific depths and how it influences the model was investigated. Table 5 lists RMSECV and R^2 of PLS models established with spectra taken at different depth ranges. For the following example, a PLS model based on two combined spectra at a depth range of 0–0.6 mm contains spectra combined from 0 and 0.2 mm, from 0.2 and 0.4 mm, and from 0.4 and 0.6 mm, i.e. the depth of the taken pairs of the spectra varies but the step size Δz of 0.2 mm remains constant. It is shown, that by using spectra at a range of depths, the prediction quality decreases compared with models using spectra from defined depths independent of the usage of combined or not combined spectra. Furthermore, the prediction quality decreases with increasing depth range. However, considering the general improvement of the prediction quality for models using combined spectra, PLS models using a preferably small depth range in combination with a high number of combined spectra (e.g. three combined spectra for a depth range of 0–0.6 mm) show comparable prediction quality compared with using models based on the combination of front and back side spectra. Thus, it is not necessary to know the absolute depth at which the spectra were taken for a higher number of combinations and whether all spectra were taken with a constant step size and within a small depth range.

4 | CONCLUSION

This study focuses on CFRP thermally damaged from one side. Depth-resolved matrix degradation (FTIR) and the development of delaminations (μCT) as well as the loss of ILSS were investigated. The resulting spectral data were analyzed with PCA regarding thermal loading. Furthermore, for predicting ILSS and delamination depth by means of infrared spectroscopy, PLS regression was applied.

It is shown that the depth of delaminations and the ILSS change with increasing thermal loading as delaminations penetrate deeper inside the CFRP and cause a decrease of ILSS. Also, the depth profiles of matrix degradation were generated by measuring with ATR-FTIR-spectroscopy along a ground incline plane. Matrix degradation occurs more pronounced near the irradiated surface and with increasing irradiation time deeper inside the CFRP.

Applying PCA on the spectral data showed that the scores were separated according to increasing thermal loading. This fact was further used to predict ILSS by means of IR spectra and PLS regression. The combination of spectra taken at different depths in the CFRP allowed for the prediction of ILSS and delamination depth by means of PLS regression even for complex parameter settings. If both sides of a CFRP structure are accessible, the simplest way of combining two spectra is taking the front and back side spectrum. This combination leads to an increase of the prediction quality compared with models using single surface spectra. The advantage of this combination is that no mechanical removal of CFRP is necessary to get spectra in different depths.

A further increase of the prediction quality can be achieved by taking spectra close to the irradiated surface and from different depths inside the specimens. Hereby, it is shown that with increasing number of combined spectra, the step size among the spectra and the depth at which the spectra were taken have less influence on the prediction quality when compared with models using single spectra. Regarding how exactly spectra have to be taken at one depth, it is shown that a reasonably good prediction is possible if spectra are taken in a certain depth range. However, the best prediction quality is achieved by using the exact depth.

For a practical application of IR spectroscopy in combination with multivariate data analysis to predict one-sided thermally induced structural damage on aircraft components in, e.g. repair processes, it is recommended to take as much spectral data as possible but also less spectral data as practically possible with a small step size close to the irradiated surface. It is important to minimize the mechanical removal because too much mechanical removal of CFRP material is counterproductive as the analysis area may potentially suffer from impaired mechanical properties, which may necessitate repair or replacement. Removing the CFRP close to the irradiated surface is advantageous because, for strong thermal loading, CFRP material must be removed anyway. In general, if external influence parameters like, for example, the sample thickness are known, models should be adjusted because an increase in prediction quality can be achieved and less combinations of the spectra and therefore less mechanical removal of CFRP is required.

ACKNOWLEDGMENT

Open access funding enabled and organized by Projekt DEAL.

ORCID

Tanja Marina Vetter https://orcid.org/0000-0001-8949-0592

REFERENCES

[1] H. Schürmann, *Konstruieren mit Faser-Kunststoff-Verbunden*, 2nd ed., Springer, Berlin, Heidelberg **2007**.
[2] A. P. Mouritz, A. G. Gibson, *Fire Properties of Polymer Composite Materials*, Springer, Dordrecht, The Netherlands **2006**.
[3] J. B. Henderson, J. A. Wiebelt, M. R. Tant, *J. Compos. Mater.* **1985**, *19*, 579.
[4] J. A. Milke, A. J. Vizzini, *J. Compos. Technol. Res.* **1991**, *13*, 145.
[5] S. Bondzic, J. Hodgkin, J. Krstina, J. Mardel, *J. Appl. Polym. Sci.* **2006**, *100*, 2210.
[6] B. Dao, J. Hodgkin, J. Krstina, J. Mardel, W. Tian, *J. Appl. Polym. Sci.* **2006**, *102*, 3221.
[7] J. Wolfrum, S. Eibl, L. Lietch, *Compos. Sci. Technol.* **2009**, *69*, 523.
[8] I. H. Dara, A. Ankara, G. Akovali, S. Suzer, *J. Appl. Polym. Sci.* **2005**, *96*, 1222.
[9] S. Eibl, *J. Compos. Mater.* **2008**, *42*, 1231.
[10] Heckner S, Geistbeck M, Grosse C U, Eibl S, Helwig A. Presented at 7th Int. Symp. NDT Aerosp. Conf. Paper, Bremen, Germany, **2015**.
[11] Shelley P, Vahey P, Werner G, Seelenbinder J. Presented at SAMPE 2011, Long Beach, CA, May 23–26, 2011.
[12] T. M. Vetter, J. Bibinger, F. Zimmer, S. Eibl, H. J. Gudladt, *J. Compos. Mater.* **2020**, *54*, 3699.
[13] G. A. Pering, P. V. Farrell, G. S. Springer, *J. Compos. Mater.* **1980**, *14*, 54.
[14] A. Ankara, B. Gökçe Dara, D. Weisgerber, *J. Thermoplast. Compos. Mater.* **2003**, *16*, 317.
[15] F. Awaja, M. T. Nguyen, S. Zhang, B. Arhatari, *Compos. Part A* **2011**, *42*, 408.
[16] H. Towsyfyan, A. Biguri, R. Boardman, T. Blumensatz, *Chin. J. Aeronaut.* **2019**, *33*, 771.
[17] V. Popow, M. Gurka, *NDT&E Int.* **2020**, *116*. https://doi.org/10.1016/j.ndteint.2020.102359.
[18] T. M. Vetter, S. Eibl, H. J. Gudladt, *Appl. Compos. Mater.* **2021**, *28*, 427. https://link.springer.com/article/10.1007/s10443-020-09865-9

[19] A. Doblies, B. Boll, B. Fiedler, *Polymer* **2019**, *11*(2), 363.
[20] R. Toivola, F. Afkhami, S. Baker, J. McClure, B. D. Flinn, *Polym. Test.* **2018**, *69*, 490.
[21] S. Eibl, J. Wolfrum, *J. Compos. Mater.* **2012**, *47*, 3011.
[22] S. Eibl, *Polym. Test.* **2019**, *76*, 396.
[23] Shelley PH, Werner GJ, Vahey PG. Applied for The Boeing Company, Patent no. US8552382B2, **2013**.
[24] J. Wolfrum, E. Whitney, S. Eibl, *J. Compos. Mater.* **2016**, *51*, 1.
[25] Werner GJ, Shelley PH, George PE. Applied for The Boeing Company, Patent no. US8044354B2, **2010**.
[26] Product Data Sheet HexPly® 8552, Hexcel Inc, www.hexcel.com.
[27] DIN EN 2563 *Carbon Fibre Reinforced Plastics – Unidirectional Laminates – Determination of the Apparent Interlaminar Shear Strength. German Version*, DIN Deutsches Institut für Normung e.V., Berlin **1997–2003**.
[28] W. Kessler, *Multivariate Datenanalyse für die Pharma-Bio- und Prozessanalytik – Ein Lehrbuch*, WILEY-VCH Verlag GmbH & Co. KGaA, Weinheim **2007**.
[29] S. Eibl, *Fire Mater.* **2011**, *36*, 309.
[30] G. Socrates, *Infrared and Raman Characteristic Group Frequencies: Tables and Charts*, 3rd ed., John Wiley & Sons Ltd, Chichester, England **2004**.
[31] L. Olivier, C. Baudet, D. Bertheau, J. C. Grandidier, M. C. Lafarie-Frenot, *Composites: Part A* **2009**, *40*, 1008.
[32] P. Musto, G. Ragosta, P. Russo, L. Mascia, *Macromol. Chem. Phys.* **2001**, *202*(18), 234.
[33] J. Wolfrum, E. Quan, G. Maier, S. Eibl, *J. Compos. Mater.* **2018**, *52*(24), 3399.
[34] S. Eibl, *Fire Mater.* **2020**, *44*, 1.
[35] J. N. Miller, J. C. Miller, *Statistics and Chemometrics for Analytical Chemistry*, 6th ed., Pearson Education Limited, Harlow, England **2010**.

How to cite this article: T. M. Vetter, F. Zimmer, S. Eibl, H.-J. Gudladt, *Polymer Composites* **2021**, *42* (8), 4138. https://doi.org/10.1002/pc.26136